

Electronic Supplementary Information (ESI)

Local Structures and TWC Activity of Pd Supported on Ni-Substituted Aluminium Oxide Borates

Yuki Nagao^{a,c}, Takafumi Hamada^a, Ayaka Imamura^a, Satoshi Hinokuma^{a,b}, Yunosuke Nakahara^c, and Masato Machida^{a,b*}

^a Department of Applied Chemistry and Biochemistry, Graduate School of Science and Technology, Kumamoto University, 2-39-1 Kurokami, Chuo, Kumamoto, 860-8555 Japan

^b Catalysts Strategic Division, Engineered Materials Sector, Mitsui Mining and Smelting Co., Ltd., 1013-1 Ageoshimo, Ageo, 362-0025 Japan

Author email address: machida@kumamoto-u.ac.jp

Fig. S1. *In situ* diffuse-reflectance FTIR spectra of adsorbed CO at 50 °C taken (a) under 1% CO/He and b) after He purging. The catalyst was reduced using H₂ at 400 °C.

Fig. S2 H₂-TPR profiles of as-prepared 0.4 wt% Pd/M-10A2B (M = Al, Mn, Fe, Co, Ni, and Cu). 5% H₂/He, 10 °C min⁻¹.

Fig. S3 TEM photographs of Pd/10A2B and Pd/Ni-10A2B after thermal ageing at 900 °C for 25 h in 10% H₂O/air.

Fig. S4 Light-off curves for NO-CO-C₃H₆-O₂ reaction over 0.4 wt% Pd supported on M-10A2B after thermal ageing at 900 °C. NO (0.050%), CO (0.510%), C₃H₆ (0.039%), O₂ (0.400%), and He (balance), *W/F* = 5.0 × 10⁻⁴ g min cm⁻³, heating rate: 10 °C min⁻¹.

Fig. S5 Pd 3d XPS spectra of Pd/10A2B (a) as-prepared, (b) thermally aged and Pd/Ni-10A2B (c) as-prepared, (d) thermally aged.

Fig. S6 Pd 3d and Ni2p XPS spectra of Pd/Ni-10A2B before and after exposure to rich environment (A/F=13.8) at 390 °C.

Fig. S7 Ni K-edge XANES of Pd/Ni-10A2B (a) before and after exposure to (b) rich environment (A/F=13.8) at 390 °C, (c) 800 °C, and (d) H₂ reduction at 800 °C.

Table S1 Reaction conditions for TWC elementary reactions.

Table S2 Fitting results for Ni K-edge EXAFS of Ni-10A2B.

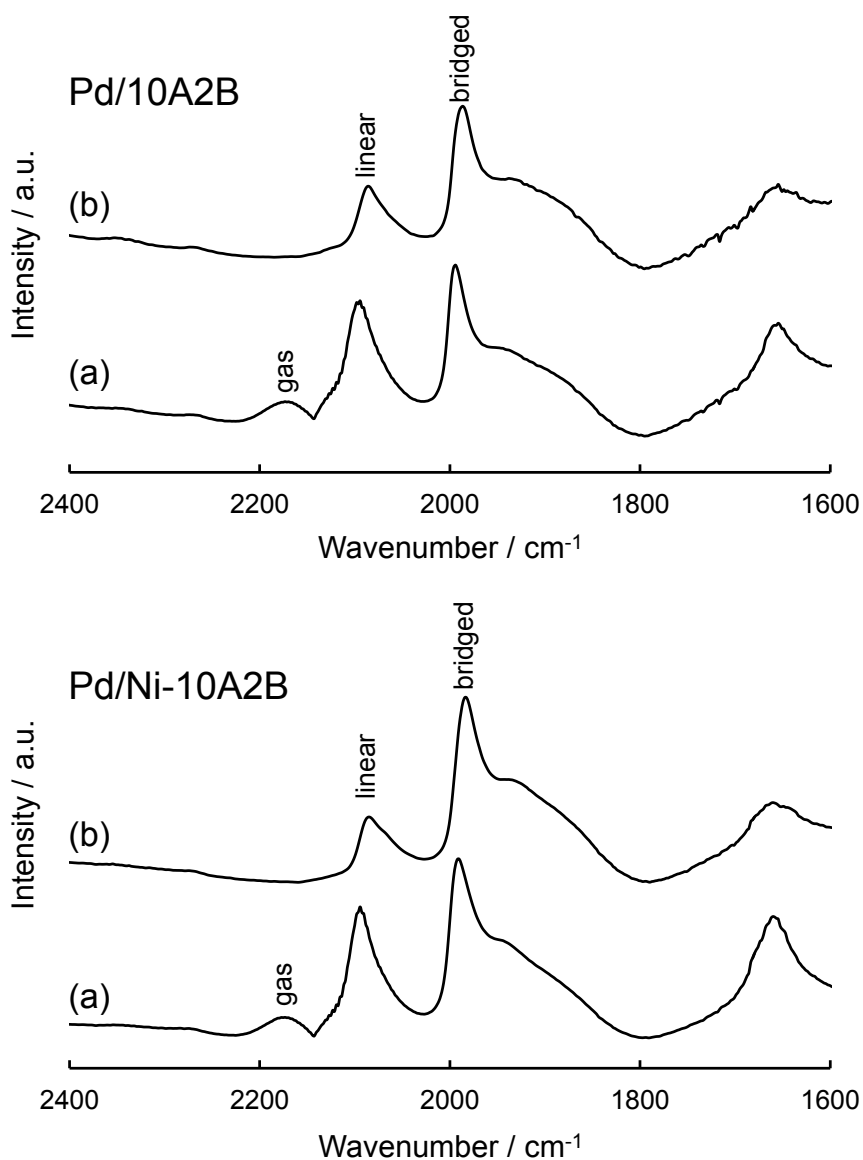


Fig. S1. *In situ* diffuse-reflectance FTIR spectra of adsorbed CO at 50 °C taken (a) under 1% CO/He and (b) after He purging. The catalyst was reduced using H₂ at 400 °C.

In situ FTIR spectra for CO chemisorption suggest that the coexistence of different chemisorption stoichiometries with linear (CO:Pd_{surf} = 1:1) and bridged (CO:Pd_{surf} = 1:2 and/or 1:3) forms. Therefore, Pd metal dispersion in the present study is expressed in terms of CO/Pd, which is a molar ratio of the CO chemisorbed per total Pd loaded.

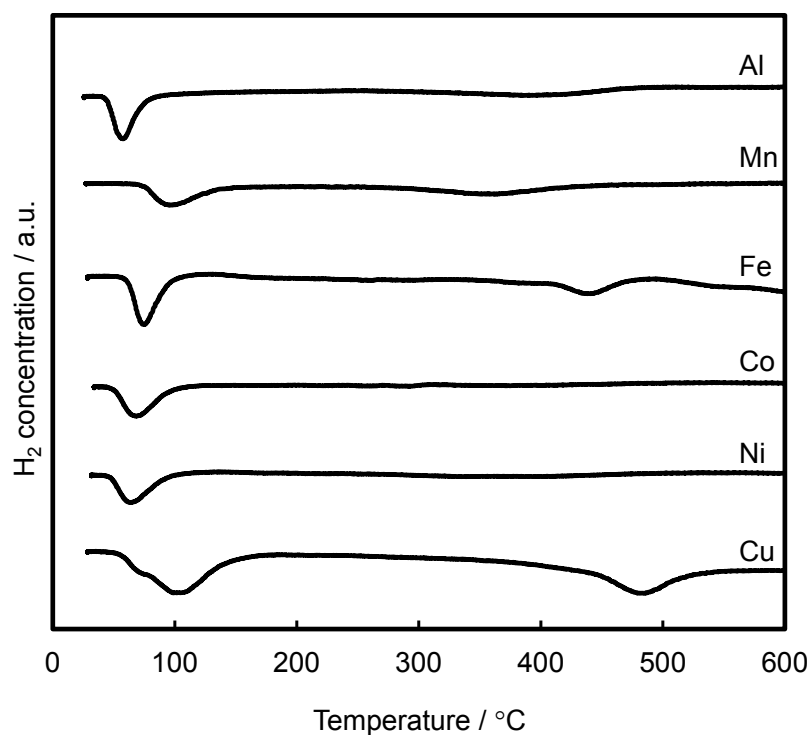
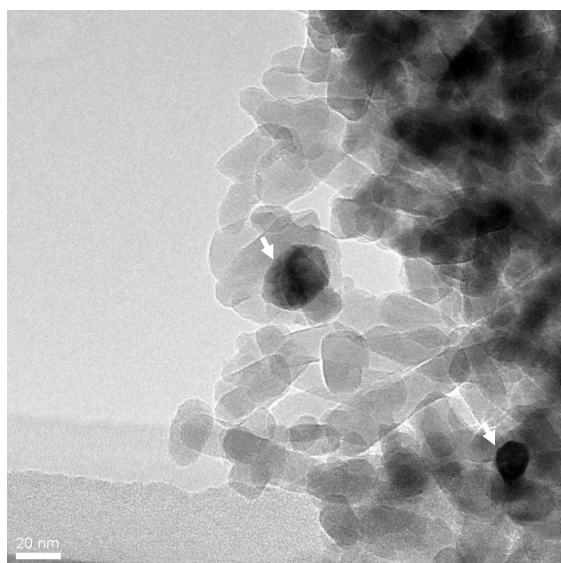


Fig. S2 H₂-TPR profiles of as-prepared 0.4 wt% Pd/M-10A2B (M = Al, Mn, Fe, Co, Ni, and Cu). 5% H₂/He, 10 °C min⁻¹.

The H₂-TPR experiments suggest Pd oxide in all samples is reduced at $T \leq 100$ °C, while the substituted 3d transition metal ions were difficult to reduce at $T \leq 500$ °C. Fe and Cu-substituted samples showed small consumptions of H₂ at 400-500 °C because of partial reduction of surface metal ions. However, most metal ions in the bulk structure were extremely stable up to 600 °C.

Pd/10A2B aged



Pd/Ni-10A2B aged

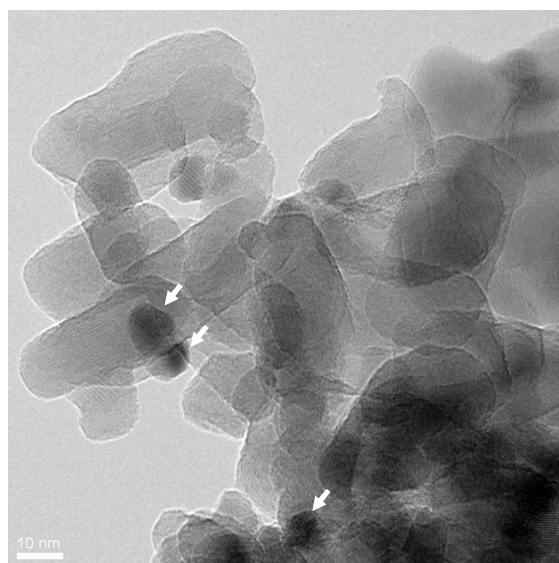


Fig. S3 TEM photographs of Pd/10A2B and Pd/Ni-10A2B after thermal ageing at 900 °C for 25 h in 10% H₂O/air.

As shown by Pd K-edge EXAFS (Fig. 4), metallic Pd was deposited after thermal ageing (900 °C, 25 h in 10% H₂O/air). In TEM images Pd metal particles grown more than 10 nm were found as shown by white arrows. These values are close to those estimated from the amount of CO chemisorbed.

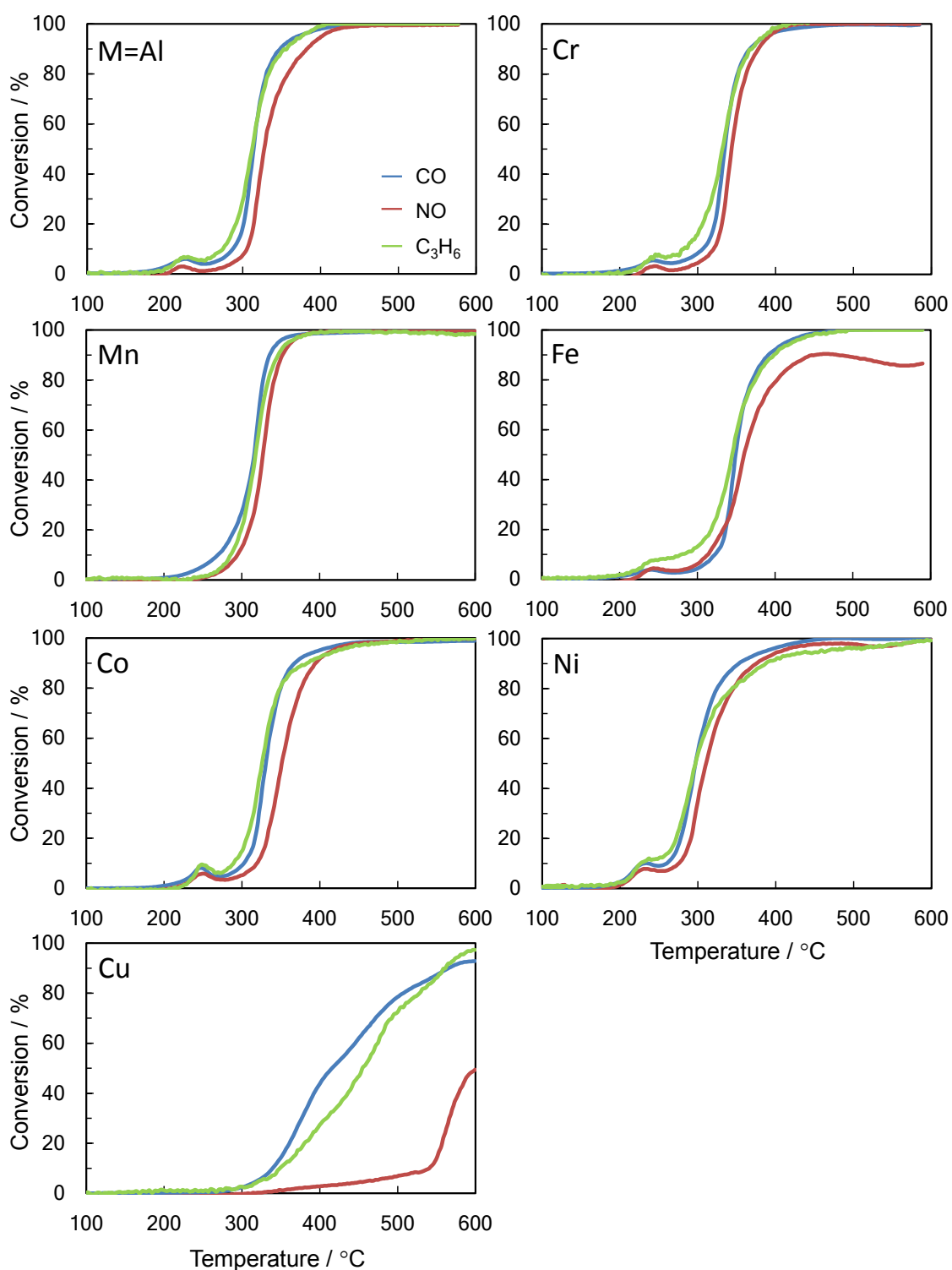


Fig. S4 Light-off curves for NO-CO-C₃H₆-O₂ reaction over 0.4 wt% Pd supported on M-10A2B after thermal ageing at 900 °C. NO (0.050%), CO (0.510%), C₃H₆ (0.039%), O₂ (0.400%), and He (balance), $W/F = 5.0 \times 10^{-4}$ g min cm⁻³, heating rate: 10 °C min⁻¹.

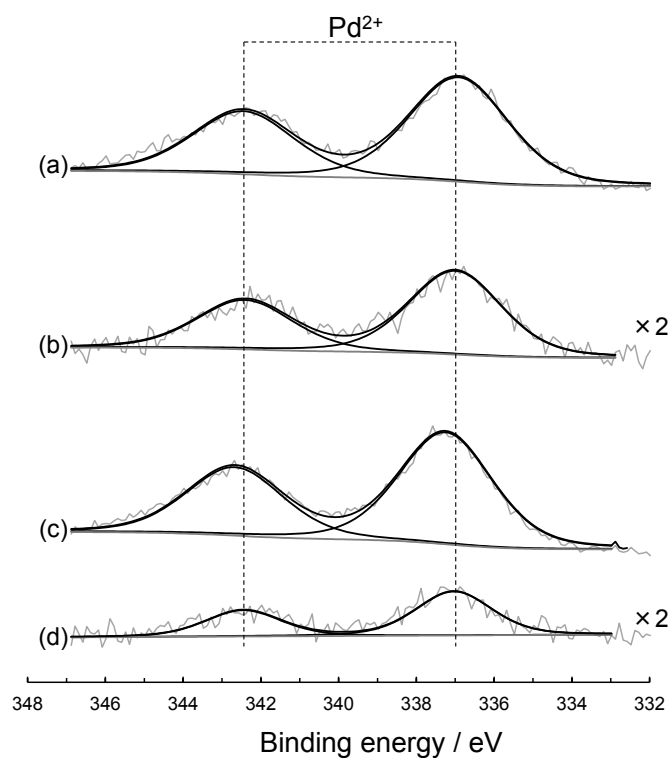


Fig. S5 Pd 3d XPS spectra of Pd/10A2B (a) as-prepared, (b) thermally aged and Pd/Ni-10A2B (c) as-prepared, (d) thermally aged.

Pd 3d XPS spectra suggest that Pd on the surface is in the divalent state before and after thermal ageing at 900 °C, although the Pd K-edge EXAFS (Fig. 4) demonstrates the thermal dissociation of PdO to metallic Pd after the thermal ageing. This discrepancy can be explained by the formation of metallic Pd particles covered by oxidised surface. Because the binding energy is almost the same for the thermally aged catalysts, the strong interactions between Pd and 10A2B or substituted Ni²⁺ can be ruled out.

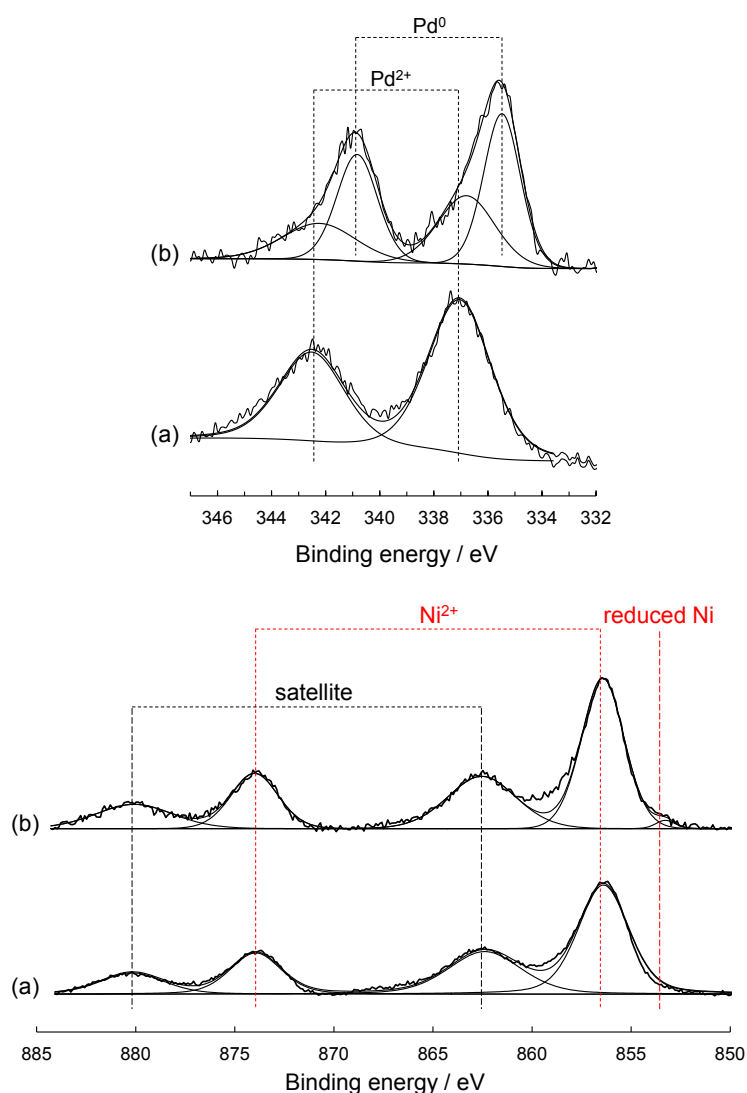


Fig. S6 Pd 3d and Ni 2p XPS spectra of Pd/Ni-10A2B (a) before and (b) after exposure to rich environment (A/F=13.8) at 390 °C.

The Pd 3d XPS spectra suggested that Pd on the thermally aged catalyst surface was fully oxidised, whereas the bulk of Pd particles was metallic as shown in Fig. 4. On exposure to a rich environment (A/F = 13.8 in Fig. 5) at 390 °C, partial reduction of Pd surface to the metallic state was observed. The Ni 2p XPS spectra suggested that Ni²⁺ was predominant in both case, although a very small peak component due to reduced Ni could be confirmed after exposure to the rich environment. However, the existence of metallic Ni (Ni⁰) can be denied because of increased CO chemisorption. In addition, Ni K-edge XANES (see **Fig. S5**) demonstrated that this treatment did not affect the overall Ni

oxidation state (Ni^{2+}). Taking these results into consideration, the observed partial reduction should be limited on the outermost surface of Ni-10A2B.

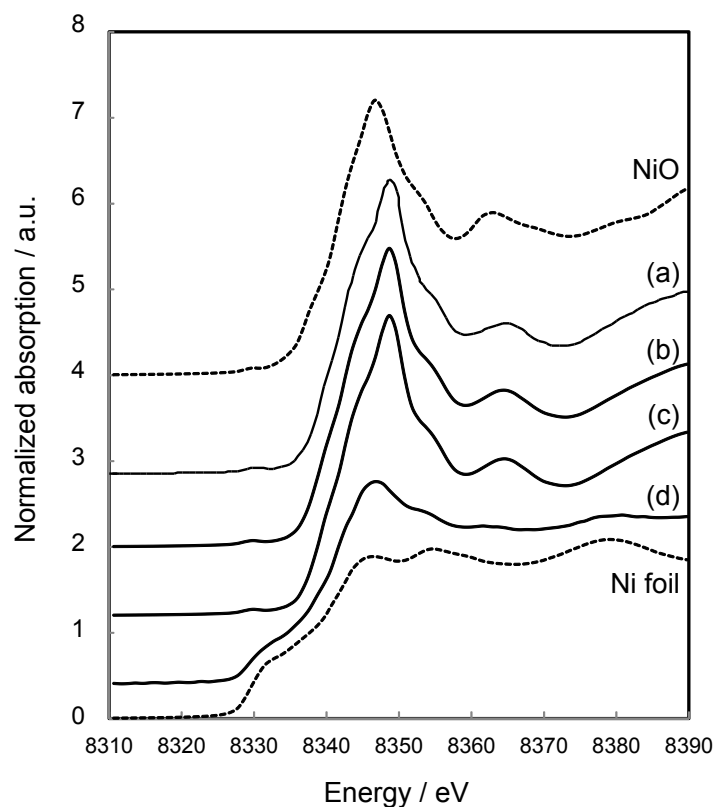


Fig. S7 Ni K-edge XANES of Pd/Ni-10A2B (a) before and after exposure to (b) rich environment (A/F=13.8) at 390 °C, (c) 800 °C, and (d) H₂ reduction at 800 °C.

The reduction of substituted Ni²⁺ ions to the metallic states was unlikely to have occurred after the Pd/Ni-10A2B catalyst was treated under rich environment (A/F = 13.8) at 390 and 800 °C as judged from shape of these spectra. By contrast, the metallic Ni was deposited to a significant extent when reduced by H₂ at 800 °C.

Table S1 Reaction conditions for TWC elementary reactions.

| | CO-O ₂ | CO-NO | CO-H ₂ O | C ₃ H ₆ -H ₂ O | C ₃ H ₆ - O ₂ | NO-C ₃ H ₆ - O ₂ | NO-C ₃ H ₆ | NO-H ₂ |
|-----------------------------------|-------------------|-------|---------------------|-------------------------------------------------|---------------------------------------------------|------------------------------------------------------|----------------------------------|-------------------|
| A/F ^a | 20.1 | 14.6 | 12.8 | 12.8 | 15.1 | 14.6 | 13.3 | 14.2 |
| λ ^b | 20.0 | 1.0 | - | - | 2.2 | 1.0 | 0.14 | 0.5 |
| CO (%) | 0.10 | 0.10 | 0.10 | | - | - | - | - |
| C ₃ H ₆ (%) | - | - | - | 0.04 | 0.05 | 0.04 | 0.04 | - |
| H ₂ (%) | - | - | - | - | - | - | - | 0.10 |
| NO (%) | - | 0.10 | - | | - | 0.05 | 0.05 | 0.05 |
| O ₂ (%) | 1.0 | - | - | | 0.50 | 0.15 | - | - |
| H ₂ O (%) | - | - | 10 | 10 | - | - | - | - |

W/F = 5.0×10^{-4} g min cm⁻³, heating rate = 10 °C min⁻¹.

^a The A/F value is calculated according to the literature¹⁴ using following excess oxygen ratio of the simulated gas feed.

$$\begin{aligned}
 \text{Excess oxygen ratio}(\lambda) &= \frac{\text{Amount of oxygen in gas feed}}{\text{Amount of oxygen required for complete oxidation}} \\
 &= \frac{2 \times p_{O_2} + p_{NO}}{9 \times p_{C_3H_6} + p_{CO} + p_{H_2}}
 \end{aligned}$$

Catalytic tests for eight TWC elementary reactions were carried out in a light-off mode as described in the main text of this manuscript.

Table S2 Fitting results for Ni K-edge EXAFS of Ni-10A2B.

| catalyst | shell | CN^a (± 0.2) | $r/\text{\AA}^b$ (± 0.03) | $\sigma^2/10^{-2} \text{\AA}^2^c$ (± 0.02) | $R/\%$ |
|----------|---------|-------------------------|------------------------------------|-----------------------------------------------------|--------|
| Ni-10A2B | Ni-O | 5.2 | 2.04 | 0.56 | 2.8 |
| | Ni-O-Al | 2.3 | 2.89 | 0.36 | 0.3 |
| | Ni-O-Al | 1.7 | 3.27 | 0.14 | 0.3 |
| | Ni-O-Al | 3.1 | 3.37 | 0.38 | 0.3 |
| | Ni-O-Al | 1.8 | 3.69 | 0.20 | 0.3 |
| NiO | Ni-O | 6.0 | 2.08 | 0.72 | 3.5 |
| | Ni-O-Ni | 12.0 | 2.95 | 0.50 | 0.3 |

Interval of k -space to r -space of FT is 3.0-16.0 \AA^{-1} .

^a Coordination number.

^b Atomic distance.

^c Debye-Waller factor.